

Supporting Materials

Selectively creating oxygen vacancies on PrCe/SiO₂ catalysts for the transformation of furfural–acetone adduct into a functionalized 1,3-diene

Yanlong Qi ^a, Shijun Liu ^{a,b}, Zaizhi Liu ^c, Long Cui ^a, Lingyun Huang ^{a,b}, Yinxin Yang ^{a,b}, Ruiyao Wu ^{a,b}, Quanquan Dai ^a, Jianyun He ^a, Wei Dong ^a, Chenxi Bai ^{a,b*}

^a Key Laboratory of High-Performance Synthetic Rubber and Its Composite Materials, Changchun Institute of Applied Chemistry, Chinese Academy of Sciences, Renmin Road, Changchun 130022, China;

^b Applied Chemistry, University of Science and Technology of China, Jinzhai Road, Hefei 230026, China.

^c College of Life Sciences, Jiangxi Normal University, Ziyang Road, Nanchang 330022, China

* Corresponding author: baicx@ciac.ac.cn

Table S1 Catalytic results over various catalysts.

Smaple	FAH concentration (%)	Conversion (%)	Selectivity (%)	Formation rate (mmol/(g _{cat} h))
SiO ₂	2	97	41	0.35
Ce/SiO ₂	2	100	92	0.81
Ce/SiO ₂	4	100	80	1.50
Ce/SiO ₂	5.3	100	59	1.51
AgCe/SiO ₂	2	100	40	0.35
LaCe/SiO ₂	2	100	75	0.61
PrCe/SiO ₂	2	100	96	0.83

Catalyst weight: 0.40 g; temperature: 300 °C; feed rate: 0.05 mL/min; N₂ flow rate: 50 mL/min;

the result data are averaged within 1 h.

Table S2 Content of CeO₂ in PrCe/SiO₂ catalysts

Smaple	CeO ₂ loading wt%
Ce/SiO ₂	12.45
PrCe _{0.42} /SiO ₂	11.58
PrCe _{0.73} /SiO ₂	11.22
PrCe _{1.07} /SiO ₂	10.87
PrCe _{1.54} /SiO ₂	10.39
PrCe _{2.11} /SiO ₂	9.68

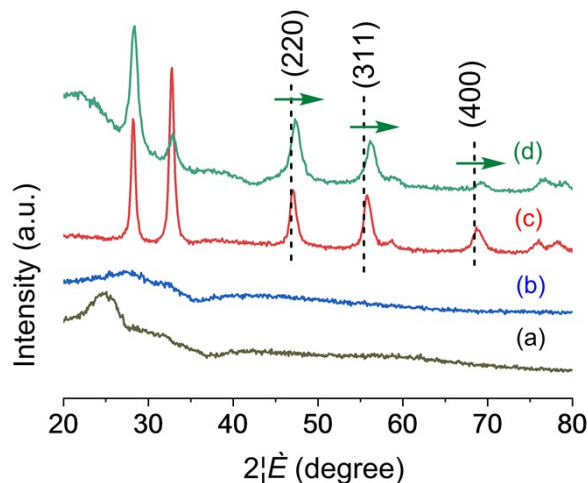


Fig.S1 XRD pattern: (a) 12wt% of Pr/SiO₂, (b) 28wt% of Pr/SiO₂, (c) Pr₆O₁₁ and (d) CeO₂

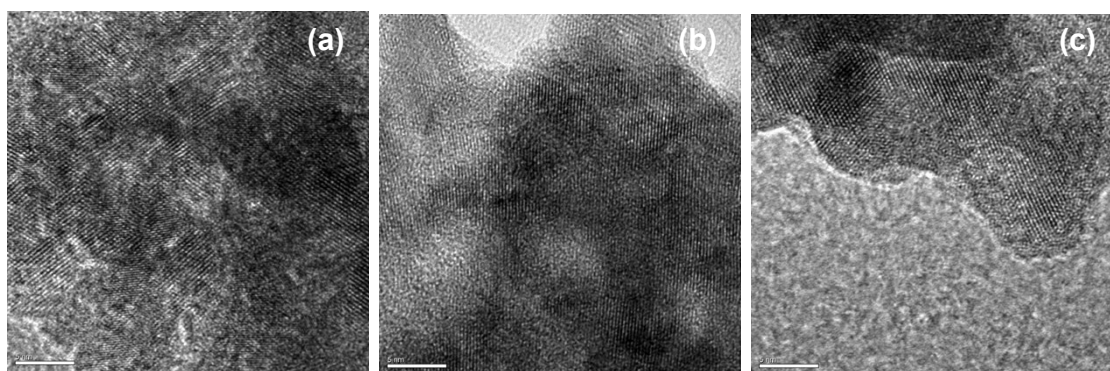


Fig.S2 HRTEM of PrCe_{1.54}/SiO₂ (a), PrCe_{2.11}/SiO₂ (b) and PrCe_{2.82}/SiO₂(c)

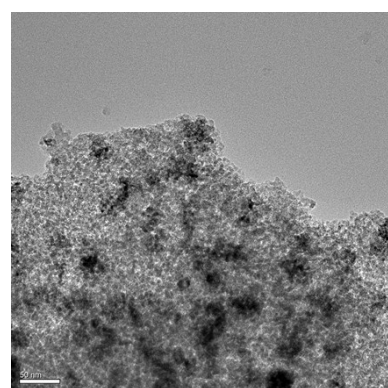


Fig. S3 TEM image of CeO₂/SiO₂

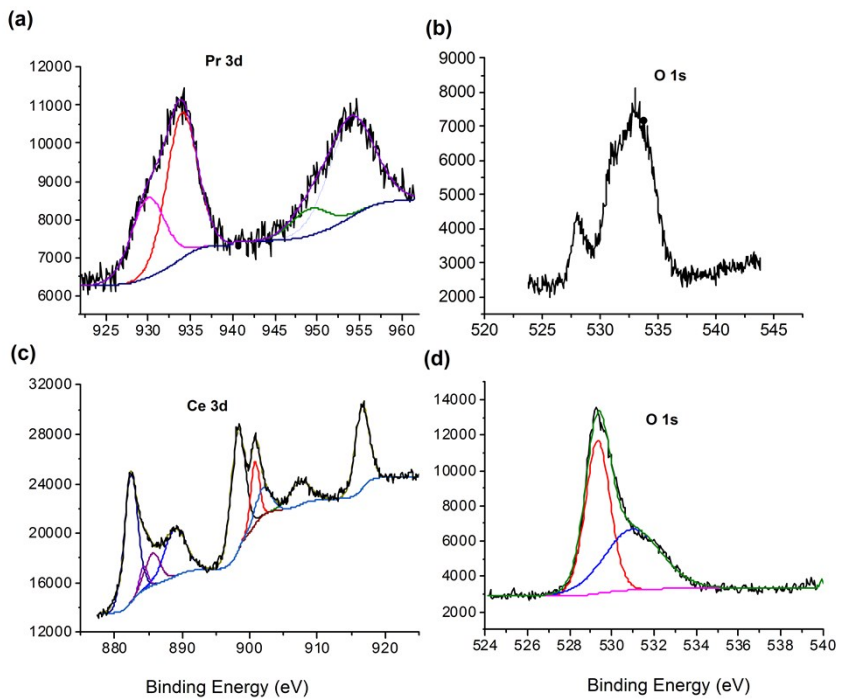


Fig. S4 XPS spectrum of pure PrO_x : (a), (b) and CeO_2 : (c), (d).

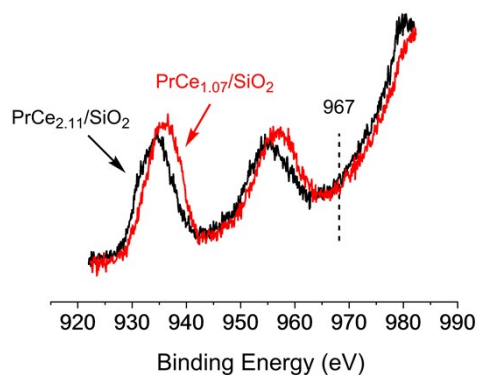


Fig.S5 XPS of Pr 3d

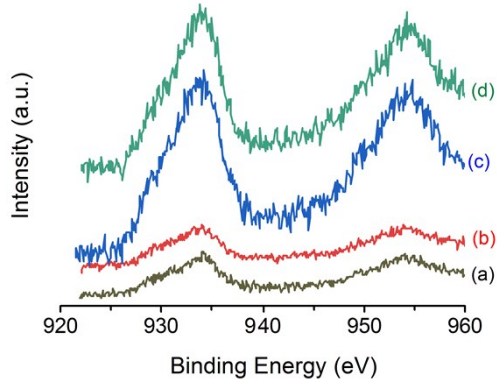


Fig. S6 XPS of Pr 3d: (a) $\text{PrCe}_{1.07}/\text{SiO}_2$, (b) $\text{PrCe}_{2.11}/\text{SiO}_2$, (c) $\text{PrCe}_{2.82}/\text{SiO}_2$, (d) Pr/SiO_2 with 28wt% of PrO_2 loading

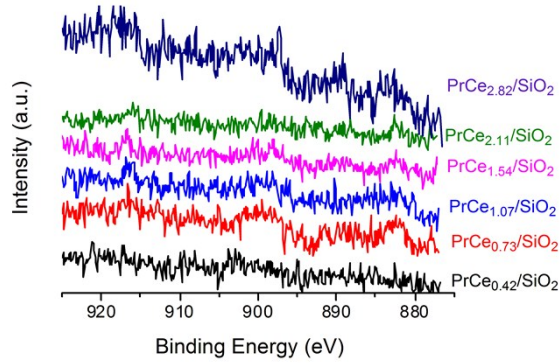


Fig. S7 XPS of Ce 3d

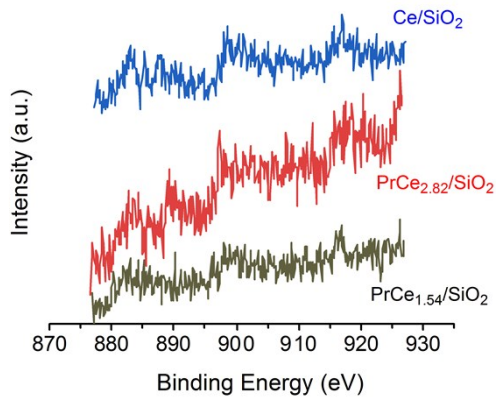


Fig. S8 XPS of Ce 3d: $\text{CeO}_2/\text{SiO}_2$ with 12.45 wt% of CeO_2 loading, $\text{PrCe}_{2.82}/\text{SiO}_2$ with 10 wt% of CeO_2 loading, and $\text{PrCe}_{1.54}/\text{SiO}_2$ with 9 wt% of CeO_2 loading.

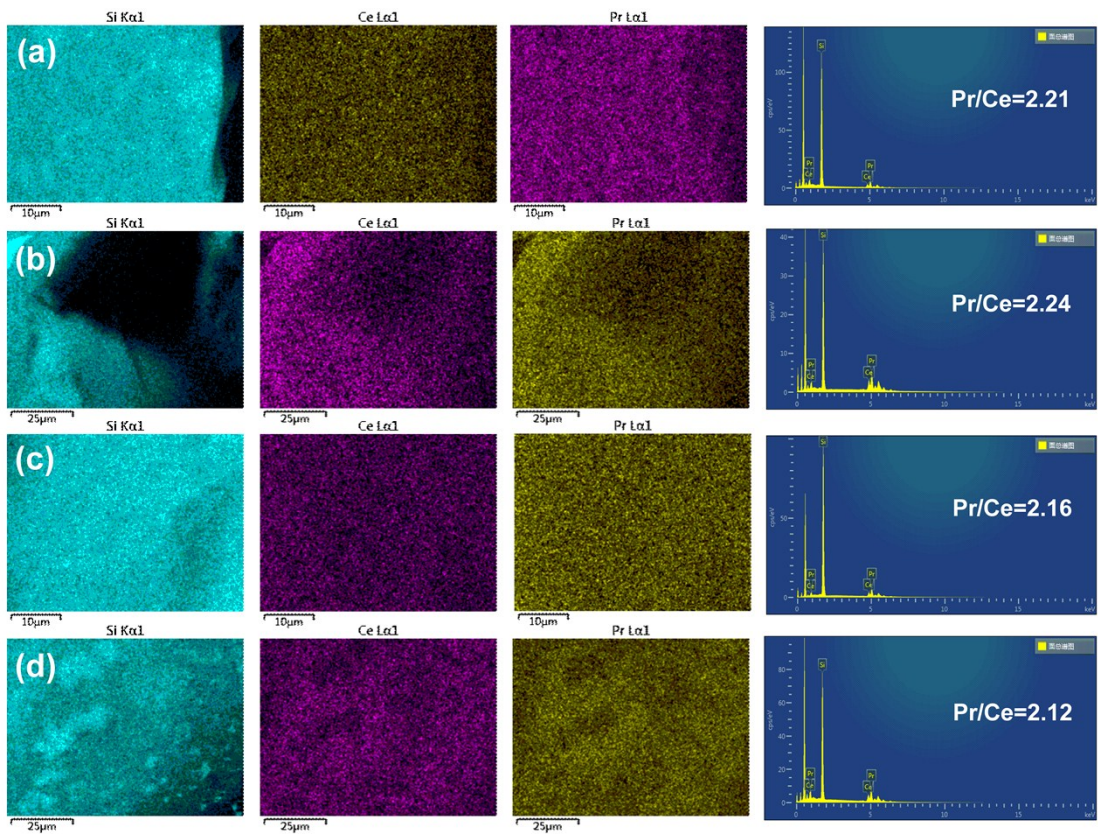


Fig. S9 SEM–EDS analysis of $\text{PrCe}_{2.11}/\text{SiO}_2$: Elemental distribution and content.

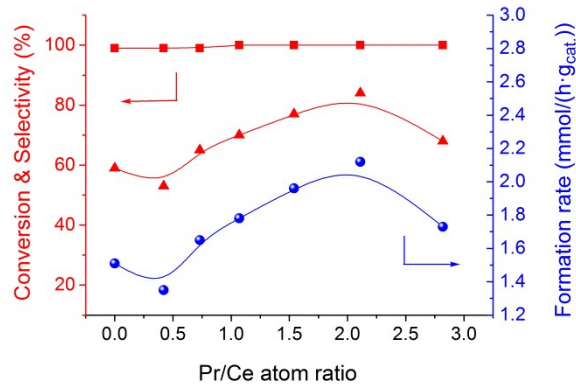


Fig. S10 Conversion, selectivity and formation rate as function of Pr/Ce atom ratio (5.3 wt% of FAH)

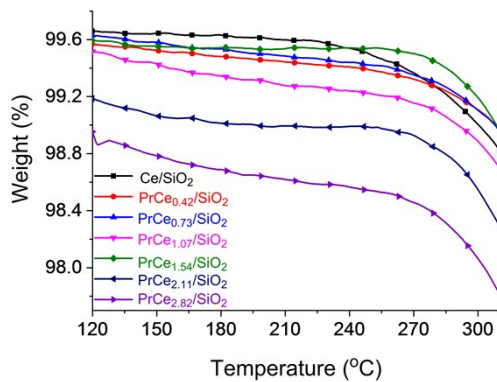


Fig. S11 TGA of spent PrCe/SiO₂ catalysts

Table S3 Relative concentration of oxygen vacancies

Smaple	$S_{OV}/(S_{OV}+S_{F2g})$
PrCe _{0.42} /SiO ₂	23
PrCe _{0.73} /SiO ₂	27
PrCe _{1.07} /SiO ₂	41
PrCe _{1.54} /SiO ₂	54
PrCe _{2.11} /SiO ₂	63
PrCe _{2.82} /SiO ₂	45

S_{F2g} : Peak area of the F2g mode at approx. 452 cm⁻¹

S_{OV} : Peak area of the oxygen vacancy at approx. 567 cm⁻¹

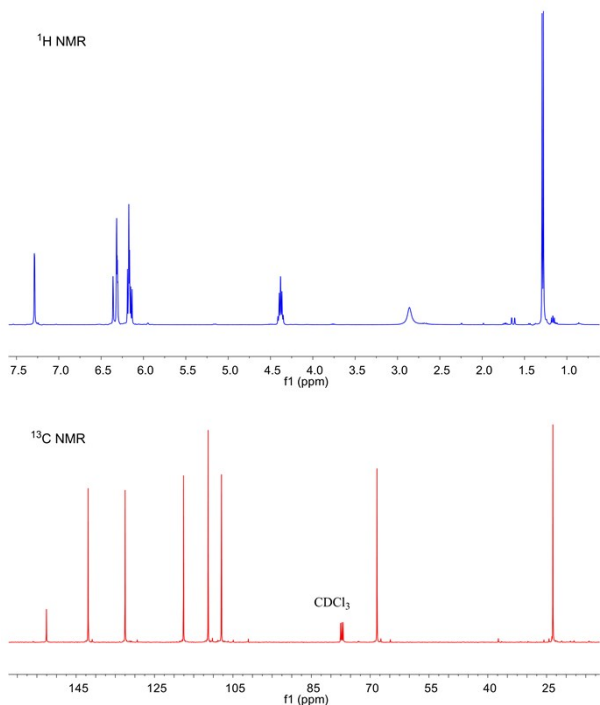


Fig.S12 ^1H NMR and ^{13}C NMR curve of FAH in CDCl_3

^1H NMR (CDCl_3 400 MHz, ppm): $\delta = 1.29$ (d, 3H), 2.86 (s, 1H), 4.38 (m, 1H), 6.10-6.22 (m, 2H), 6.26-6.39 (m, 2H), 7.29 (d, 1H).

^{13}C NMR (CDCl_3 100 MHz, ppm): $\delta = 23.40, 68.25, 107.92, 111.33, 117.61, 132.49, 141.93, 152.56$

Ref: *Org. Lett.* 2012, **14**, 5134-5137; *J. Org. Chem.* 2010, **75**, 2981-2988; *J. Mol. Catal. B: Enzym.* 2016, **126**, 37-45; *J. Org. Chem.* 1987, **52**, 4855-4859

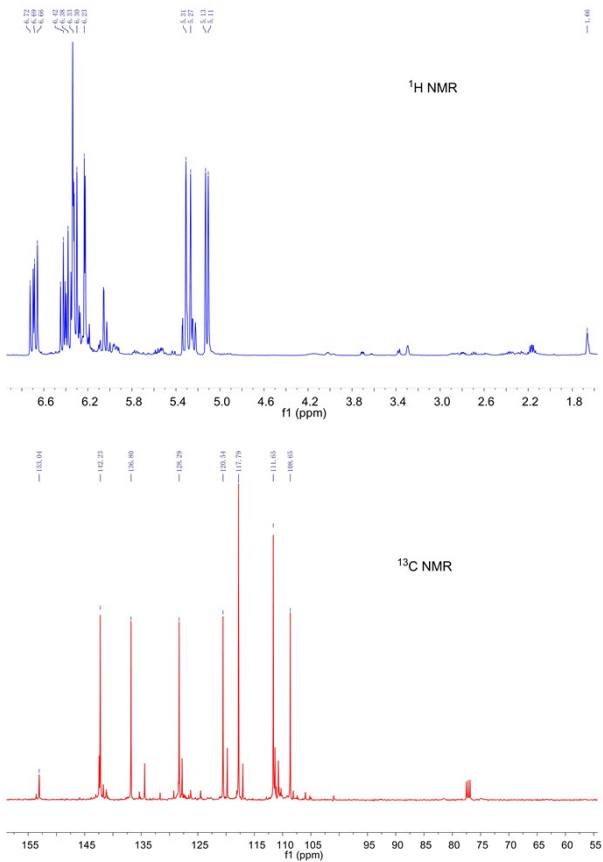


Fig.S13 ¹H NMR and ¹³C NMR curve of F-diene in CDCl₃

¹H NMR (CDCl₃ 400 MHz, ppm): δ = 7.37 (d, 1H), 6.72 (dd, 1H), 6.47-6.26 (m, 3H), 6.23 (d, 1H), 5.31 (d, 1H), 5.13 (d, 1H).

¹³C NMR (CDCl₃ 100 MHz, ppm): δ = 153, 142, 136, 128, 120, 117, 111, 108

Ref: *Org. Biomol. Chem.*, 2010, **8**, 2312-2315; *Chem. Commun.*, 2018, **54**, 10104-10107; *Chem. Eur. J.* 2013, **19**, 3833-3837.